

Electron Paramagnetic Resonance and Computational Studies of Radicals Derived from Boron-Substituted N-Heterocyclic Carbene Boranes

John C. Walton,^{*,†} Malika Makhlof Brahmī,[‡] Julien Monot,^{‡,§} Louis Fensterbank,[‡] Max Malacria,[‡] Dennis P. Curran,^{*,§} and Emmanuel Lacôte^{*,‡,||}

[†]School of Chemistry, EaStChem, University of St. Andrews, St. Andrews, Fife KY16 9ST, United Kingdom

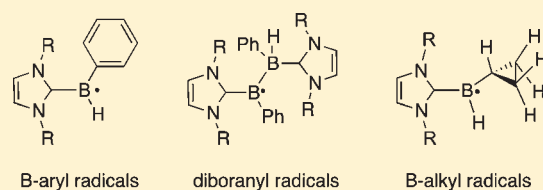
[‡]UPMC Univ Paris 06, Institut parisien de chimie moléculaire (UMR CNRS 7201), C. 229, 4 place Jussieu, 75005 Paris, France

[§]Department of Chemistry, University of Pittsburgh, Pittsburgh, Pennsylvania 15260, United States

S Supporting Information

ABSTRACT: Fifteen second-generation NHC-ligated boranes with aryl and alkyl substituents on boron were prepared, and their radical chemistry was explored by electron paramagnetic resonance (EPR) spectroscopy and calculations. Hydrogen atom abstraction from NHC–BH₂Ar groups produced boryl radicals akin to diphenylmethyl with spin extensively delocalized across the NHC, BH, and aryl units. All of the NHC–B·HAR radicals studied abstracted Br-atoms from alkyl bromides. Radicals with

bulky *N,N'*-dipp substituents underwent dimerization about 2 orders of magnitude more slowly than first-generation NHC-ligated trihydroborates. The evidence favored head-to-head coupling yielding ligated diboranes. The first ligated diboranyl radical, with a structure intermediate between that of ligated diboranes and diborenes, was spectroscopically characterized during photolysis of di-*t*-butyl peroxide with *N,N'*-di-*t*-butyl-imidazol-2-ylidene phenylborane. The reactive site of B-alkyl-substituted NHC–boranes switched from the boron center to the alkyl substituent for both linear and branched alkyl groups. The β -borylalkyl radicals obtained from *N,N'*-dipp-substituted boranes underwent exothermic β -scissions with production of dipp-Imd–BH₂· radicals and alkenes. The reverse additions of NHC–boryl radicals to alkenes are probably endothermic for alkyl-substituted alkenes, but exothermic for conjugated alkenes (addition of an NHC–boryl radical to 1,1-diphenylethene was observed). A cyclopropylboryl radical was observed, but, unlike other α -cyclopropyl-substituted radicals, this showed no propensity for ring-opening.



INTRODUCTION

Recent research has revealed that N-heterocyclic carbene boranes (NHC–borane) possess novel features that make them significantly different from boranes, borohydrides, and even other borane–Lewis base complexes.¹ NHCs are strong electron-pair donors, so their complexes with boranes are remarkably stable as compared to borane sulfides, ethers, and even amines. NHC-ligated trihydroborates (NHC–BH₃) are precursors for unusual boryl radicals,² borenium cations,³ boryl anions,⁴ and borylenes.⁵ NHC–BH₃ complexes are robust and stable to ambient conditions and to chromatography; hence they are also finding use as synthetic reagents in radical,⁶ ionic,⁷ and organometallic reactions.⁸ They are also promising co-initiators in radical photopolymerizations.⁹

The B–H bonds of NHC–boranes are dramatically weaker than in uncomplexed boranes,¹⁰ having $\Delta H^\circ(\text{B–H})$ values of 80–88 kcal mol^{−1} according to ab initio computations^{2,11,12} and experimental studies.¹³ Consequently, NHC–boryl radicals were easily generated by H-atom abstraction from a first-generation of complexes with the NHC ligated to BH₃ (Figure 1). Conventional radical initiators, including *t*-butoxyl,¹⁴ triplet benzophenone,⁹ and C-centered radicals,¹⁵ abstract H-atoms from NHC–BH₃ at rates that depend strongly on the steric shielding at the boron center by

the NHC substituents. The resulting NHC–boryl radicals (NHC–BH₂·) have π -delocalized structures, very different from the σ -electronic structures of amine–boryl and phosphine–boryl radicals.^{11,16}

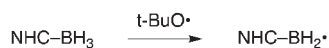
Opportunities to alter properties by changing the NHC substituent are plentiful, so the NHC groups were extensively modified during this prior work on first-generation NHC–boranes.^{9,14,15} Yet the boron substituent was constant (BH₃). Substituents on the boron atoms are anticipated to both modify the steric environment about B and perhaps change the strength of the B–H bonds. Novel chemistry is therefore expected for a second generation of complexes substituted at boron (NHC–BH₂R).

Here, we prepare and study 15 NHC–boranes with a range of aryl and alkyl substituents on boron. H-abstraction is rapid for B–Ar complexes, but the reactivity of the resultant B-aryl substituted radicals is strikingly low in dimerizations. The chemistry of B-alkyl NHC–boranes is influenced by a trade-off between substituents on the NHC rings and the B-alkyl substituents, with radicals sometimes being generated by C–H abstraction (from the alkyl substituent)

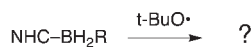
Received: April 26, 2011

Published: May 28, 2011

first-generation: NHC widely varied, BH₃ held constant (ref. 2)



second-generation: NHC is imidazol-2-ylidene, R substituent varied



R = aryl, alkyl

Figure 1. First- (ref 2) and second-generation (this work) NHC–borane radical precursors.

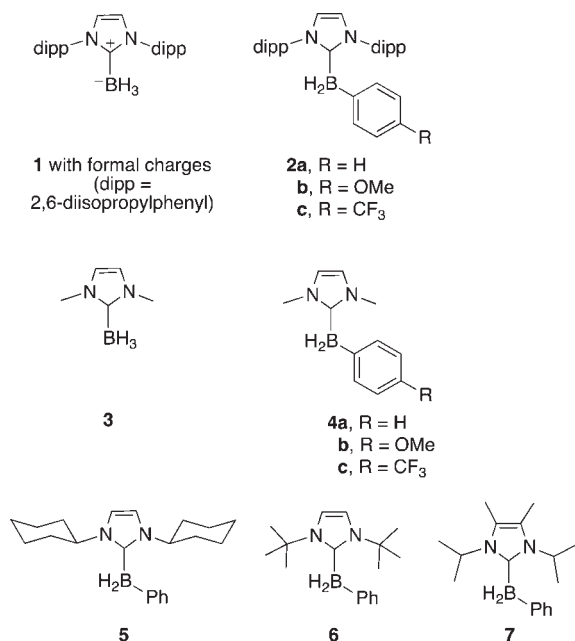


Figure 2. Structures of N-heterocyclic carbene boranes for study of B–Ar substitution. Formal charges are shown on 1 for illustration. The corresponding NHC–BH₂· and NHC–B·HAr radicals are designated as 1·, 2a·, etc.

and sometimes by B–H abstraction. The structures and onward reactions (by themselves, with each other, and with alkyl bromides) of all of these different radicals are described.

RESULTS AND DISCUSSION

NHC–Boranes with B-Aryl Substituents. Figure 2 shows the structures of two first-generation standards (1 and 3) and nine aryl-substituted NHC–boranes that were prepared to probe the effects of B-aryl groups. In a previous report,¹⁴ the standard imidazol-2-ylidene boryl radical 1· with large N-dipp substituents was much longer-lived and far less reactive than analogue 3· with small N–Me groups. The set of NHC–boranes 2a–c was intended to reveal the effect of B-aryl substituents with electron-releasing and electron-withdrawing properties on comparatively crowded and long-lived intermediates. By way of contrast, NHC–boranes 4a–c were chosen to yield analogously substituted but transient NHC–boryl radicals. Compounds 5–7 were selected to probe the combined effect of B-phenyl and imidazo-lylidene ring substituents. All of the B–Ar compounds are readily

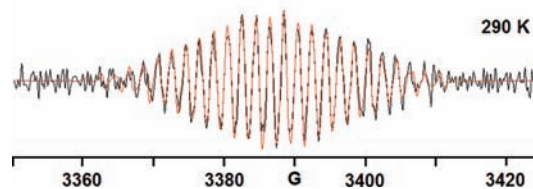
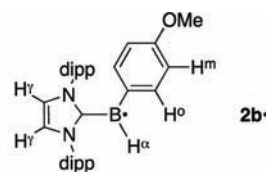


Figure 3. Structure and overlay of the experimental (black) and computer-simulated (red) EPR spectra of NHC–B·HC₆H₄OMe-4 radical (2b·) in PhH at 290 K.

available from boronic acids by a recently published route,¹⁷ and details for their preparation and characterization are provided in the Supporting Information.

Deaerated solutions of individual NHC–boranes and di-*tert*-butyl peroxide (DTBP) in *tert*-butylbenzene or benzene were irradiated with UV light in the resonant cavity of a 9 GHz EPR spectrometer. We expected that the photochemically generated *t*-BuO· radicals would abstract hydrogen from the BH₂ groups of the substrates, thus generating the NHC–B·HAr radicals. Satisfactory spectra were obtained from each of 2a–c. Figure 3 shows the structure and spectrum of 2b·; the spectra of the radicals derived from 2a and 2c are in the Supporting Information.

The EPR parameters obtained from computer simulations of the spectra are listed in Table 1. The ¹¹B and H^α hyperfine splitting constants (hfs) of 2a·–2c· are smaller than for the standard radical 1·, indicating that spin density is delocalized away from the B-atom into the phenyl rings. In line with this, hfs from phenyl ring H-atoms were resolved for 2a· and 2c· and partly for 2b·. The trend in the magnitudes of *a*(¹¹B) roughly corresponds with the mesomeric effects of the *para*-substituents (Hammett σ_p constants of H, OMe, and CF₃ being 0.0, –0.16, and 0.53, respectively).¹⁸

The structure of radical 2a· was computed by DFT employing the UB3LYP functional with the 6-31G+(d) basis set,¹⁹ and this is shown in Figure 4 along with the computed SOMO. The planes of the 2,6-diisopropylphenyl rings are virtually perpendicular to the plane of the imidazole ring and hence out of conjugation. This agrees with the lack of hfs from the dipp-ring H-atoms in the EPR spectra. The computed hfs were in reasonable agreement with experiment (Table 1) apart from *a*(¹¹B).²⁰ The structure (Figure 4) shows that even with the *i*-Pr groups rotated as far away as possible, the steric shielding of the B-atom is considerable. The planes of the Ph and imidazole rings are disposed at an angle to each other of only about 15°. Thus, the SOMO that extends across these two rings and the BH unit is practically a pure π -system. The computations imply these radicals are boron analogues of diphenylmethyl (Ph₂CH·) and that (like diphenylmethyl) resonance stabilization is very significant.

The additional resonance stabilization in radicals 2· favors H-atom abstraction from the parent NHC–BH₂Ar reagents. However, the extra steric shielding of the B-atom as compared to parent NHC–BH₃ 1 opposes the approach of the *t*-BuO· radical. To assess the effect of aryl substitution on the H-atom donor ability of 2a–c, competitive H-abstractions were carried out with propan-2-ol. UV irradiation of solutions containing the NHC–borane and propan-2-ol, together with DTBP, gave rise to EPR

Table 1. Experimental and Computed EPR Parameters for Aryl-Substituted NHC–Boryl Radicals^a

NHC–boryl	T/K or basis set ^b	$a(1H^\alpha)$	$a(11B)$	$a(2N)$	$a(2H^\gamma)$	$a(2H^\delta)$	$a(2H^m)$	$a(H^p)$
1 ^c	300	11.4(2H)	7.3	4.0	1.0			
2a ^c	300	9.3	6.6	3.9	2.8	1.1	1.1	2.8
2a ^c	6-31G+(d) ^d	-9.7	11.6	3.6, 3.4	-1.4, -0.7	-2.0	0.9	-2.4
2b ^c	290	9.8	5.9	3.8	1.6	1.6	nr ^e	
2c ^c	295	9.6	6.9	4.2	1.8	1.8	0.8	^f

^a All g -factors 2.0028 ± 0.0005 ; hfs in gauss. Note that only the magnitudes and not the signs of hfs can be derived from EPR spectra. ^b DFT computations with the UB3LYP functional; geometry optimized with the 6-31G+(d) basis set. ^c Data from ref 13. ^d Computations with the EPR-iii basis set failed. ^e nr = not resolved. ^f Possibly $a(3F) = 0.8$ G; correlation coefficient virtually unchanged on including this.

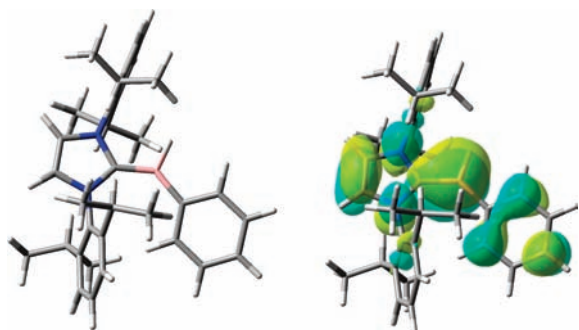


Figure 4. DFT computed structure (left) and SOMO (right) of NHC–boryl radical 2a[·].

spectra showing both the NHC–boryl radical and the 2-hydroxypropan-2-yl radical. Stock solutions of known concentrations of each of 2a, 2b, or 2c together with DTBP were prepared. To each was added a known amount of propan-2-ol, and then the EPR spectrum was recorded during photolysis. The ratio of the concentrations of the two radicals was obtained from spectral simulations. The spectra were relatively weak, so only rough estimates of the ratios of the two radicals could be obtained (see the Supporting Information for spectrum from 2b).

To analyze these data, it is easily shown that $k_H/k_H^s = [\text{NHC–B} \cdot \text{HAr}][i\text{-PrOH}]/[\text{Me}_2\text{C} \cdot \text{OH}][\text{NHC–BH}_2\text{Ar}]$, where k_H refers to H-atom abstraction from the NHC-borane by $t\text{-BuO} \cdot$ and k_H^s refers to the propan-2-ol standard. From a sample containing excess propan-2-ol to 2a (molar ratio 47:1), the measured ratio of the derived radicals was 2a[·]:Me₂C·OH about 6:1; hence $k_H/k_H^s \approx 280$. For 2b, $k_H/k_H^s \approx 230$. Spectra from 2c were too weak for analysis. The rate constant for H-atom abstraction from propan-2-ol by $t\text{-BuO} \cdot$ is $1.8 \times 10^6 \text{ M}^{-1} \text{ s}^{-1}$ at 295 K;²¹ hence the k_H values at 295 K for 2a and 2b are about 5×10^8 and $4 \times 10^8 \text{ M}^{-1} \text{ s}^{-1}$, respectively. These are marginally larger than the k_H of the unsubstituted parent 1 ($k_H = 1.4 \times 10^8$ at 295 K).¹³ Apparently, the additional resonance stabilization conferred on the NHC–boryl radicals by the aryl substitution marginally outweighs the increased steric shielding in these H-abstractions with alkoxy radicals.

Alkyl radicals also abstract H-atoms from unsubstituted carbene boranes.^{13,15} These rate constants are much lower (10^4 – $10^5 \text{ M}^{-1} \text{ s}^{-1}$), but the reactions are still important in preparative radical chain reductions. To assess the effect of a phenyl substituent on such reactions, we used a published method^{15,22} to estimate the rate constant of a primary-alkyl radical (nonyl) with 2a. At $<10^4 \text{ M}^{-1} \text{ s}^{-1}$, the rate constant was below the lower limit of the experimental method. In contrast, the rate constant for reaction of a primary-alkyl radical with 1 is somewhat above the limit at $(2\text{--}4) \times 10^4 \text{ M}^{-1} \text{ s}^{-1}$.^{13,15} While it is not clear how much less reactive 2a is

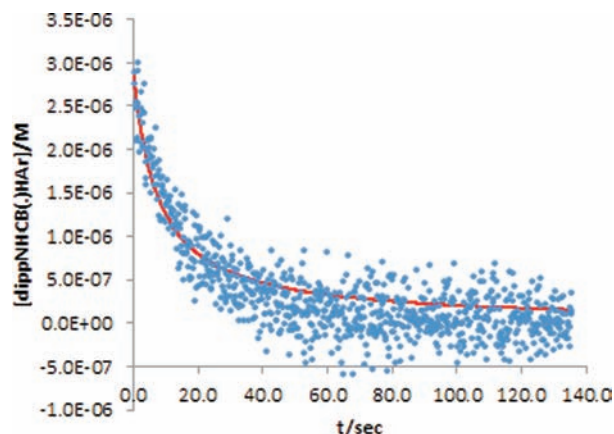


Figure 5. Decay of the EPR signal of radical 2c[·] as a function of time at 300 K. Blue: Experimental data points. Red: Second-order line for $2k_t = 4.5 \times 10^4 \text{ M}^{-1} \text{ s}^{-1}$.

toward alkyl radicals than 1, it is clear that 2a is not a promising reagent for radical chain reductions involving alkyl radicals. Apparently, for the slow reactions of alkyl radicals with 2a, the steric shielding of the phenyl group outweighs its resonance stabilization.

The kinetics of the termination processes of the dipp-Imd–B·HAr radicals were investigated by following the decays of their EPR signals as functions of time. Samples of each of the dipp-Imd–boranes and DTBP were prepared in PhH and degassed, and then the radicals were generated as before. The EPR magnetic field was fixed in turn at the maximum intensity of the signal of each radical. The decays of the signals were then monitored as a function of time on shuttering the UV photolysis beam. Several separate samples were examined, and a typical curve is shown in Figure 5 for the decay of 2c[·] at 300 K.

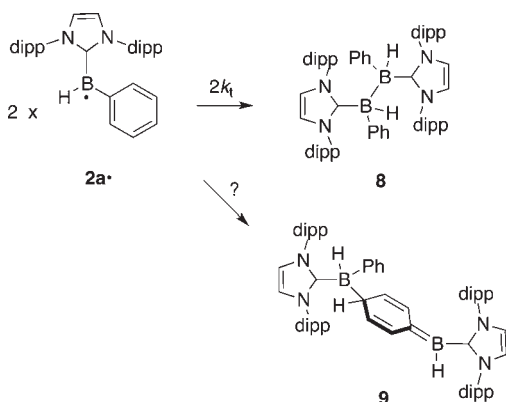
The initial concentrations of the dipp-Imd–B·HAr radicals were determined from the average of the double integrals of the full spectra before and after photolysis. The decays could not be satisfactorily fitted by first-order plots, but reasonably good fits were obtained for second-order decays having the $2k_t$ values listed in Table 2. The fits were slightly imperfect (see Figure 5 and Supporting Information), suggesting that there may be a first-order contribution to the decay. The half-lives of the dipp-Imd–B·HAr radicals are about 10 s. Therefore, a combination of the dipp-Imd–B·HAr radicals with $t\text{-BuO} \cdot$ radicals cannot be the process that is first order in dipp-Imd–B·HAr in the dark because all of the $t\text{-BuO} \cdot$ radicals must react within a few milliseconds of shuttering the UV beam.

Table 2 shows that the termination rate constant for the *B*-phenyl-substituted radical 2a[·] is more than 2 orders of magnitude smaller than $2k_t$ for the unsubstituted radical 1[·] dipp-Imd–BH₂·.

Table 2. Termination Rate Constants for dipp-Imd–Boryl Radicals^a

radical	B-substituent	temp/K	[NHC–BH ₂ ·] _i /M ^b	2 <i>k</i> _t M ⁻¹ s ⁻¹
1·	H	300	5.1 × 10 ⁻⁷	9.0 × 10 ⁶
2a·	Ph	292	3.6 × 10 ⁻⁶	5.0 × 10 ⁴
2b·	4-MeOC ₆ H ₄	292	2.1 × 10 ⁻⁶	3.8 × 10 ⁴
2c·	4-CF ₃ C ₆ H ₄	300	2.9 × 10 ⁻⁶	4.5 × 10 ⁴

^a In PhH solution except 1·, which was in PhBu-*t*. ^b Initial concentration of dipp-Imd–boryl radical.

Scheme 1. Possible Terminations of Phenyl-Substituted Radical 2a·

We suggest that radical 2· terminates by dimerization in a head-to-head fashion to give 8.¹⁴ Dimer 8 is a ligated diborane analogous to compounds NHC–BH₂–BH₂–NHC that have been recently reported by Robinson.²³ We suggested that first-generation radical 1a· terminates to make a diborane,¹³ and recently Braunschweig has observed such a dimer.⁵ The Ph substituent in 2a· imposes additional shielding on both partners in a head-to-head combination reaction yielding dimer 8, which probably explains the large decrease in rate of termination of 2a· as compared to 1a·.

Matsumoto and Gabbai have reported that an electrochemically generated NHC–B·(mesityl)₂ radical (mesityl = 2,4,6-trimethylphenyl) is highly persistent,³ so much so that they even attempted to obtain an X-ray structure. So we considered that termination might take place by coupling of the boron center of one radical with the *para*-site of the phenyl ring in the second radical to give head-to-tail dimer 9 as shown in Scheme 1. This type of coupling is subject to less steric hindrance than head-to-head coupling and predominates in the terminations of triphenylmethyl and related radicals.

To assess this possibility, we studied 4-methoxy- and 4-trifluoromethyl-substituted radicals 2b· and 2c·. Like Matsumoto and Gabbai's radical, the *para*-positions in these radicals are blocked to shut off head-to-tail dimerization. The 2*k*_t values for 2b· and 2c· are very similar to 2*k*_t for the phenyl derivative 2a· (Table 2), so we conclude that only head-to-head coupling to yield dimer 8 occurs. Accordingly, the extreme persistence of Matsumoto and Gabbai's radical is not primarily due to the *para*-methyl groups on the two mesityl rings. The reluctance of boron to form double bonds to carbon is well documented,²⁴ and this may explain why head-to-tail dimers like 9 are not formed.

Radical generation from aryl-substituted NHC–boranes 4a–c and 5–7 was also examined, but no well-defined EPR signals could

Table 3. Relative EPR Signal Intensities from Reactions of NHC–Boryl Radicals with 1-Bromobutane and 2-Bromo-2-methylpropane^a

	3·	4a·	4b·	4c·	5·	7·	1·	2a·	2b·	2c·
<i>n</i> -Bu·	3.4	1.2	0.4	0.6	1.8	1.6	0.6	0.06	0.06	0.00
<i>t</i> -Bu·	1.0	0.8	0.5	0.3	1.0	0.9	2.2	0.5	0.3	0.4

^a Determined from the double integrals of the EPR spectra of the *n*-Bu· or *t*-Bu· radicals relative to the *t*-Bu· radical intensity obtained from 3·.

be obtained from any of these precursors (except 6; see below). There are probably two reasons for this. First, the corresponding NHC–boryl radicals may all be transient because the alkyl-substituted imidazole N-atoms provide less steric shielding to termination by dimerization than in 2a–c·. So radical concentrations are low. Second, because the interaction of the unpaired electron with the H-atoms of N-alkyl groups is significant,¹⁴ the spectrum of radical 4a· (NCH₃) could be divided into as many as 2160 lines. Individual resonance lines from 4a· (and the others in the series 4b, c, 5–7) could therefore be below the noise level.

To learn whether boryl radicals were being generated by H-abstraction from these NHC-boranes, we added 1-bromobutane or 2-bromo-2-methylpropane to EPR samples prior to irradiation. Abstraction of halogen atoms from alkyl halides by boryl radicals has been observed before by EPR spectroscopy,¹⁴ by laser flash photolysis,⁹ and in preparative experiments.²⁵ Indeed, all of the NHC-boryl radicals derived from 4a–c, 5–7 abstracted bromine from alkyl bromides to some extent, and the relative intensities of the *n*-Bu· and *t*-Bu· radical spectra observed are shown in Table 3.

The initial reactant concentrations and reaction conditions were essentially the same for all of these experiments so the relative intensities (that is, the yield of *n*-Bu· or *t*-Bu·) are related to the overall efficiency of the bromine abstraction. However, the relative intensities will also depend on the rates of termination reactions. Table 3 shows that the yield of *n*-Bu· was highest for the least shielded radical 3· and lowest for most shielded radicals 2a–c·, with the other radicals giving intermediate yields. Consistent with this, LFP studies show that 3· is more reactive toward 1-iodopropane than 2·. The picture is less clear for the *t*-Bu· series. The spread of values is comparatively less, and the sterically congested radicals 1· and 2a–c· gave appreciable yields of *t*-Bu·. This can possibly be attributed to a slower cross-combination of the larger *t*-Bu· with the congested NHC–boryl radical.

In addition to this evidence, in parallel studies we have observed radicals 4a· and 4b· by LFP experiments.^{10b} We conclude that boryl radicals can be generated to some extent by H-atom abstraction from precursors 4a–c, 5, and 7, but that these radicals must be relatively short-lived. In contrast to the restrained behavior of these *N*-methyl, *N*-isopropyl, and *N*-cyclohexyl substrates, irradiation of *N*-*t*-butyl substrate 6 rewarded us with a big surprise.

A Unique Diboranyl Radical. Samples of di-*t*-Bu–Imd–borane 6 in PhH with DTBP were irradiated, and in time strong spectra were obtained; however, these spectra (Figure 6) exhibited four unusual features: (1) the strong signals took several minutes to develop; (2) the hyperfine splitting pattern was substantially greater in extent than that of the other NHC–boryls; (3) only extremely weak *n*-Bu· and *t*-Bu· spectra were observed when alkyl bromides were added; and (4) decay of the radical species was much slower than anticipated. From measurements of the initial radical concentration and decay curve fitting, a second-order rate constant of 2*k*_t = 6 × 10⁵ M⁻¹ s⁻¹ was obtained at 280 K. The decay was also

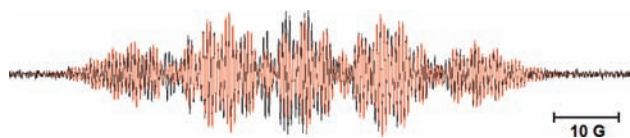


Figure 6. Overlay of the experimental (black) and simulated (red) EPR spectra obtained from photolysis of DTBP and **6** in PhH at 300 K.

monitored at 300 K, and the data were more scattered, but the same rate constant was derived. These factors suggested a different kind of radical was produced from **6** and that this radical had more steric shielding around the B-atom than the expected radical **6**.

A satisfactory computer simulation of the spectrum was eventually obtained with the parameters shown in Table 4. The EPR parameters show couplings to two N-atoms, two H-atoms, and one B-atom with magnitudes suggesting the presence of an NHC–B· unit. In addition, the three hfs of 2.8 G (*ortho* and *para* H-atoms) and two of 0.6 G (*meta* H-atoms) show the unpaired electron is also delocalized into a phenyl ring. There remain a coupling to a second B-atom and one comparatively large coupling to an H-atom. These data suggest that the observed species is the ligated diboranyl radical **11** (Scheme 2 and Figure 7) with one H^β.

We suggest that radical **11** is formed by H-atom abstraction from dimer **10**. In turn, this is produced during photolysis by combination of the initial radicals **6**·, so the delay in the development of the signal is sensible. Similarly, the greater extent of steric shielding in **11** as compared to **6**· explains the slow decay and reluctance to abstract Br-atoms.

NHC-ligated diboranes are unusual species that have recently been identified by Robinson and co-workers from the reduction of NHC–BBr₃ with potassium/graphite in THF.²³ Rare diboranes of type NHC–BH=BBH–NHC were also produced from the same reactions. These were thermally stable, although air- and moisture-sensitive. We now find that neutral diboranyl radical **11**, which represents an intermediate stage between a diborene and a diborane, is also a viable species with a half-life of ~1 s in solution. Unlike all of the other NHC–boranyl radicals of this study, **11** contains a labile β-H-atom; hence termination could take place by disproportionation to re-form ligated diborene **10** together with an equal amount of the novel ligated diborene **12**. Dimerization to yield ligated tetraborane **13** also is possible (Scheme 2). Radical **11** can be viewed as the adduct from H-atom addition to diborene **12** (or indeed as the adduct from Ph· radical addition to a diborene of structure NHC–BPh=BBH–NHC). The structures of several neutral and anionic diboranes with aromatic and aryloxy substituents have been reported,²⁶ but the chemistry of ligated diboranes is in its infancy.²⁷ Our results suggest analogies with alkenes are appropriate.

The computed structure of **11m** shows the NHC–B·B unit as virtually planar with the Ph–B· ring twisted somewhat out of this plane (dihedral 44°). The imidazole and Ph rings attached to the BH center are orthogonal, in agreement with their lack of hfs in the EPR

spectrum. The SOMO is a π-type orbital (Figure 7) spanning the NHC–B·(Ph)BH moiety. The calculated B–B bond length of 1.756 Å is nicely intermediate between the observed (X-ray) values of 1.561 and 1.828 Å for the NHC-ligated diborene NHC–BH=BBH–NHC and diborane NHC–BH₂–BH₂–NHC, respectively.²³ The B–H^β bond length and BBH^β bond angle of **11m** are 1.233 Å and 105.0°, respectively. The computations show that the B^β–H^β bond made an angle of 23° with the plane of the SOMO at B^β. This, together with the extensive π-spin delocalization, explains why the *a*(H^β) is somewhat smaller than the maximum permitted value (about 20 G). The computed H^β hfs (and the hfs of the H's in the PhB· ring) are very sensitive to the dihedral angles subtended with the SOMO. Considering the comparative ease of rotation about the single bonds involved, the agreement of calculation with experiment (Table 4) is impressive.

NHC–Boranes with B-Alkyl Substituents. We previously showed that H-abstraction from *tert*-butyl borane **14** by *t*-BuO·

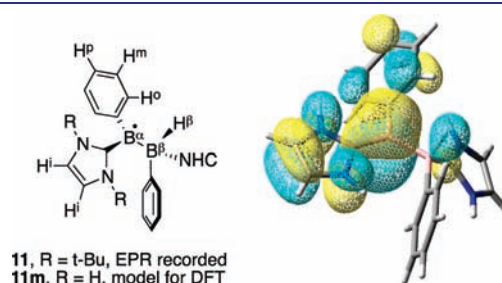


Figure 7. Structures of radicals **11** and **11m** (left), and DFT computed structure and overlaid SOMO of model diboranyl radical **11m** (H-atoms replace *t*-Bu groups on the imidazole rings of **11**).

Scheme 2. Formation and Decay of Ligated Diboranyl Radicals

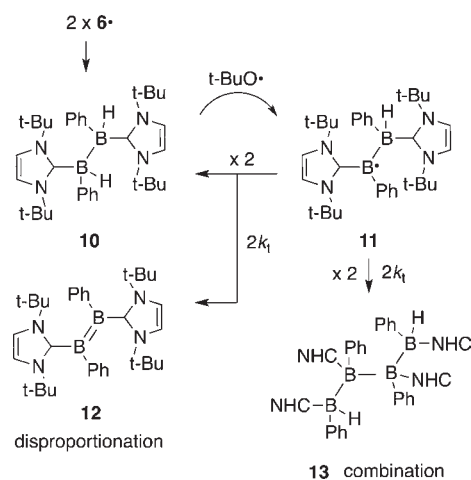


Table 4. EPR Parameters of Ligated Diboranyl Radical **11**^a

radical	T/K or DFT basis set	<i>a</i> (¹¹ B ^α)	<i>a</i> (H ^β)	<i>a</i> (¹¹ B ^β)	<i>a</i> (2N)	<i>a</i> (2H ⁱ)	<i>a</i> (3H ^{o,p})	<i>a</i> (2H ^m)
11	300	11.7	11.2	3.4	3.4	2.4	2.8	0.6
model 11m ^{b,c}	6-31G+(d)	14.4	15.1	−5.3	3.3	−0.8, −1.2	−1.0, −1.2, −1.5	0.6
model 11m ^{b,c}	6-311+(d,p)	5.5	14.9	−4.8	2.3	−0.8, −1.1	−1.0, −0.9, −1.3	0.5

^a *g*-factor 2.0030 ± 0.0005; hfs in gauss. Only the magnitudes and not the signs of hfs can be derived from EPR spectra. ^b Model **11m** as **11** but H replaces *t*-Bu on N-atoms of the imidazole rings. ^c DFT computations with the UB3LYP functional; geometry optimized with the 6-31G+(d) basis set. Hfs for all other Hs were computed to be ≤ ±0.1 G (except the NHs). Computations with the EPR-iii basis set failed.

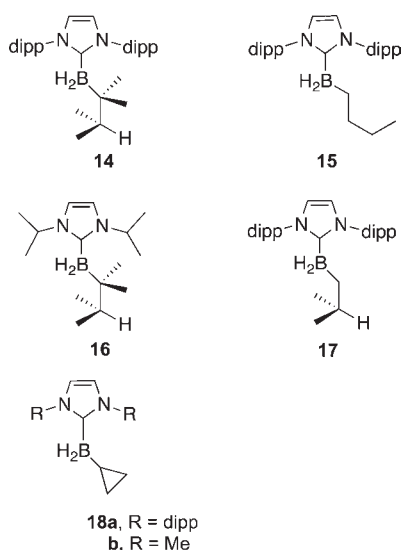


Figure 8. The NHC–boranes with B-alkyl substituents studied.

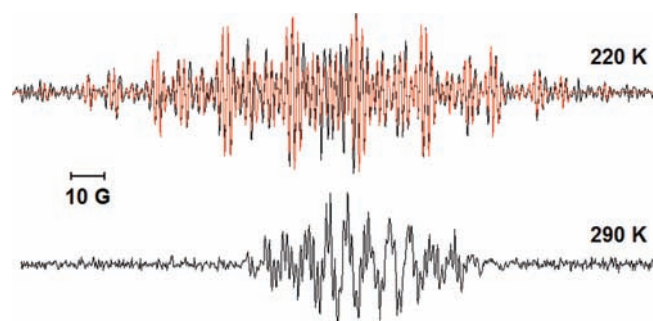


Figure 9. Top: Overlay of computer simulation (red) and experimental (black; after digital removal of broad central feature) EPR spectra obtained from **17** in *t*-BuPh at 220 K. Bottom: EPR spectrum from **17** at 290 K (identified as NHC–boryl **1**·).

radicals takes place selectively at the tertiary H-atom of the hexyl group.¹⁴ The C-centered radical generated in this way undergoes β -scission to give 2,3-dimethylbut-2-ene and the dipp-Imd–BH₂· radical **1**·. To more generally assess the regioselectivity of H-atom abstraction from B-alkyl–NHC–boranes, new compounds **15**–**18** were investigated (Figure 8; see Supporting Information for preparation and characterization details).

Surprisingly, when a solution containing *n*-butyl precursor **15** and DTBP in *t*-BuPh was photolyzed in the EPR resonant cavity, the only detectable species in the temperature range 220–290 K was parent radical **1**·. *t*-BuO· radicals are normally unselective in abstracting from hydrocarbon chains. Thus, we expected that an assortment of the C-centered radicals from abstraction of all types of secondary H-atoms of the butyl chain might be formed along with the NHC–B·HBu-*n* radical. That only **1**· was detected suggests that CH₃CH₂CH·CH₂BH₂–NHC was selectively formed and subsequently dissociated to give **1**· and 1-butene. We tried to observe the C-centered radical at low temperature, but the spectra were broad and poorly resolved.

When the isobutyl precursor **17** was examined, the complex EPR spectrum shown in the top of Figure 9 was obtained at low temperatures (<220 K) in *t*-BuPh solvent. On raising the temperature, this spectrum weakened and was replaced above

about 240 K by a new spectrum. This sharpened at 290 K to the spectrum shown in the bottom of Figure 9. This is the spectrum of previously reported NHC–boryl radical **1**·.

We attempted to record spectra at lower temperatures in cyclopropane, but these were ill-defined and weak, probably because of poor solubility of **17**. Computer simulation of the 220 K spectrum provided the EPR parameters shown in Table 5. Comparison of these data with those reported for radical **20b**¹⁴ suggested that the 220 K spectrum belonged to C-centered radical **20a**. This conclusion was supported by the results of a DFT computation with model radical **19** bearing *N*-methyl substituents (Figure 10 and Table 5). It follows that the *t*-BuO· radical selectively abstracts the tertiary H-atom from the isobutyl group in preference to one of the BH₂ hydrogens. At higher temperatures, radical **20a** undergoes β -scission, thus releasing NHC–boryl **1**· and isobutene (see Scheme 3).

The EPR spectra were too weak for radical concentration measurements, but we estimated by visual inspection and simulation that radical **20a** and the released radical **1**· were of equal concentration at about $T_{\text{mid}} = 210$ K. The activation energies (E_d) of many unimolecular reactions correlate with EPR-derived T_{mid} values according to eq 1:²⁸

$$E_d/\text{kcal mol}^{-1} = 0.044T_{\text{mid}} + 0.22 \quad (1)$$

Accordingly, $E_d = 9.5$ kcal mol⁻¹ for the β -scission of **20a**. Strictly, this linear correlation is only expected to hold for processes in which the rearranged and unrearranged radicals terminate at the diffusion-controlled limit. The ejected radical **1**· undergoes dimerization more slowly than this, but termination may be dominated by the much faster cross-combination with **20a**. So the value obtained from eq 1 is probably reasonably reliable. Assuming a normal pre-exponential factor of 10¹³ s⁻¹, the rate constant k_d for the β -scission of **20a** at 300 K is about 10⁶ s⁻¹.

The estimated E_d value compares well with the $E_d = 8.1$ kcal mol⁻¹ previously obtained for dissociation of **20b**.¹⁴ The higher activation energy for β -scission of **20a** is as expected because the isobutene released is less stable than the 2,3-dimethylbut-2-ene released from **20b**. The process is fast for both radicals, which accords well with the idea that NHC-ligation weakens B–C bonds as well as B–H bonds.¹¹

Evans–Polanyi equations relating the activation energies of β -scission reactions to the overall reaction enthalpies (ΔH°) have been obtained.²⁹ A basic relationship derived for hydrocarbon radicals and ignoring polar effects is:

$$E_d (\text{kcal mol}^{-1}) = 12.4 + 0.79\Delta H^\circ \quad (2)$$

The estimated reaction enthalpies derived from use of eq 2 with the E_d data for **20a**,**b** indicate both dissociations are exothermic by 4–5 kcal mol⁻¹! This was unexpected because NHC–boryl radicals add rapidly (by experiment) and irreversibly (by calculation) to methyl acrylate.⁹ The rapid addition is key to the success of NHC–boranes as co-initiators in radical photopolymerization. NHC–boryl radicals are nucleophilic,^{9,25} so polar effects operating in the transition state favor addition to methyl acrylate and not isobutene. Yet could the additions of NHC–boryl radicals to simple alkenes really be endothermic? We turned to calculations to independently address the reaction enthalpies.

A DFT computational study of the closely related model radical **19** was undertaken with the UB3LYP functional and a 6-31G+(d) basis set.¹⁴ The reaction coordinate for the β -scission of **19** to NHC–boryl **3**· and isobutene was followed by incrementation of the B–C bond while allowing all other geometrical parameters to

Table 5. EPR, Kinetic, and Thermodynamic Data for NHC–Bora-alkyl Radicals

radical	T/K or DFT basis set	$a(6H^\beta)/G$	$a(2H^\beta)/G$	$a(^{11}B)/G$	$a(2H^\gamma)/G$	T_{mid}/K	$E_d/kcal/mol$	$k_d/s^{-1}300 K$	$\Delta H^\circ/kcal/mol$	ref
20a ^a	220	21.1	13.1	19.3	1.5	210	9.5	10^6	−3.8	this work
19	6-31G+(d)	19.6	11.6	20.2	−1.6		7.8		−4.0	this work
20b	155	20.8		16.0		180	8.1	10^7	−5.4	14

^a In PhBu-*t* solution; $g = 2.0027$.

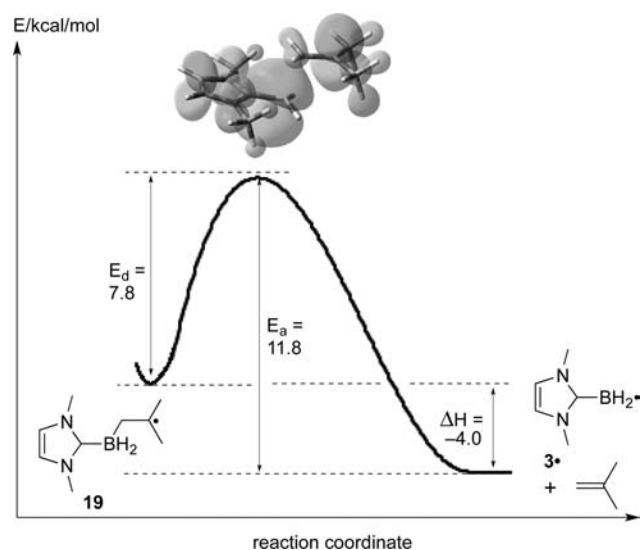
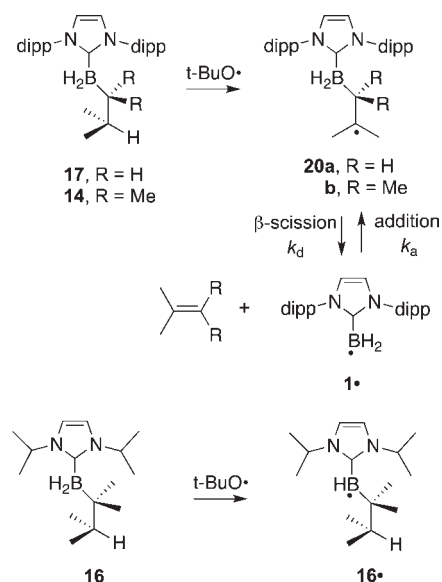


Figure 10. DFT reaction coordinate and transition state for β -scission of model radical **19**.

Scheme 3. β -Scission of Isobutyl–NHC–Borane **20a**



relax. The B–C bond lengthened from its initial value of 1.683 to 2.230 Å in the transition state (TS) (Figure 10).

The computed HOMO of the TS showed that there was extensive delocalization of the unpaired electron into the π -system of the NHC–boryl unit. This supports the idea that resonance stabilization of NHC–boryl radicals is an important contributing factor to their

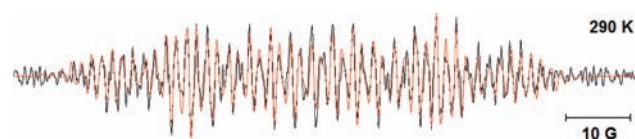


Figure 11. Overlay of simulated (red) and experimental (black) EPR spectra of **21** obtained from addition of **3•** to 1,1-diphenylethene in PhH at 290 K.

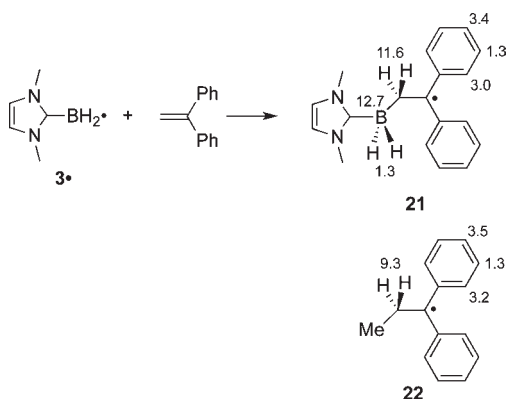
ready formation in this reaction (and others).¹¹ The energies of the reactant, products, and TS were corrected for their zero point energies and for thermal effects to 298 K (Table 5). The DFT results supported the finding of exothermic β -scission, and the magnitudes of the calculated activation energy and reaction enthalpy were in pleasing agreement with the experimental values obtained for radical **20a** (Table 5 and Figure 10).

These β -scissions are, of course, the reverse of NHC–BH₂• radical additions to alkenes and have the same TSs. The B–C–C angle of approach of **3•** to isobutene was computed to be 104.3°. For additions of C-centered radicals to various types of alkenes, the computed C–C–C angles of approach lie in the alkyl carbon range 106–112°, and the lengths of the forming C–C bonds are between 2.17 and 2.31 Å.^{30,31} These values are not very different from the B–C–C angle and B–C bond length that we calculated for dissociation of **19**. However, addition of **3•** to isobutene was computed to be endothermic by 4 kcal mol^{−1}, and the addition activation energy was 11.8 kcal mol^{−1} (close to the experimental value of 13.3 kcal mol^{−1}). C-centered radicals provide a stark contrast. For example, the experimental activation energy for addition of methyl radical to isobutene is only 6.2 kcal mol^{−1}, and the reaction is exothermic by 19.5 kcal mol^{−1}.^{30,31}

The resonance-stabilized benzyl radical has been suggested as a model for NHC–boryls.^{11,13} Experimental data for addition of benzyl radical to isobutene are not available, but data for its addition to other alkenes show the activation energy to be about 9 kcal mol^{−1} for an exothermic reaction.³⁰ We conclude that NHC–boryl radical additions to unactivated alkenes are inherently slower than are C-centered radical additions and that atom transfer addition reactions to such alkenes (that is, radical hydroborations) may be difficult to accomplish. On the other hand, addition/elimination reactions³² of assorted radicals to B-allyl or B-alkenyl substituted NHC–boranes could well be feasible.

To further ascertain whether boryl radicals are inclined to add to alkenes, we examined the EPR spectra from photolyses of solutions containing the most reactive NHC–borane **3**, DTBP, and several different alkenes including cyclohexene and acrylonitrile. However, only weak and/or ill-defined signals were obtained. Reasoning that addition might occur if the energy of the product radical were lowered by significant resonance stabilization, we investigated the reaction of **3•** with 1,1-diphenylethene. This produced the EPR spectrum shown in Figure 11.

Scheme 4. EPR hfs (ν /G) of Adduct Radical **21** with Model α -Ethyldiphenylmethyl Radical



The EPR parameters derived from the simulation are displayed on structure **21** in Scheme 4. Comparison of these hfs with those of α -ethyldiphenylmethyl **22**,³³ which serves as a model, supports the conclusion that addition takes place to afford β -borylalkyl radical **21**. We conclude that although NHC–boryls do not readily add to alkyl-substituted alkenes, addition can take place at ambient temperature to alkenes with substituents that provide significant resonance stabilization in the adduct radical.

Compound **16** containing a B-thexyl group combined with N-*i*-Pr substituents provided a pivotal comparison with compound **14** containing B-thexyl and N-dipp substituents. To our surprise, reaction of **16** with *t*-BuO \cdot radicals gave the spectrum of the corresponding B-centered radical **16 \cdot (see the Supporting Information and Table 6). In **14**, the dipp substituents shield the boron center to such an extent that H-abstraction at the tertiary H-atom of the thexyl group is preferred. Similar behavior is observed for **15** and **17**, reinforcing the conclusion that this is due to the N-substituent, not the B-substituent (which is bulky in **14** but not in **15** or **17**). On the other hand, in **16**, steric shielding by the *i*-Pr substituents is much less important and H-abstraction at the weaker B–H bonds proceeds. This is an outstanding example of the steric regio-switching that can be accomplished by means of NHC scaffolds (Scheme 3).**

Ring-opening is the defining reaction of cyclopropylcarbonyl and related radicals (cyclopropyloxy, cyclopropylaminyl),³⁴ so we wondered whether cyclopropylboryl radicals would open. Hydrogen abstraction from the cyclopropyl-substituted precursor **18a** by *t*-BuO \cdot radicals gave a good quality EPR spectrum (see the Supporting Information) that was analyzed as shown in Table 6. This spectrum was essentially unchanged in the range of 170–350 K. Upon addition of 1-bromobutane or 2-methyl-2-bromobutane, the spectra of the corresponding alkyl radicals were observed. These results are good evidence that radical **18a \cdot has formed.**

Analyzing the EPR spectrum, the hfs to boron (4.5 G in **18a \cdot) is significantly smaller than observed for other NHC–boryl radicals (see, for example, Table 1). The HOMO of cyclopropane is a degenerate pair of orbitals constructed from p-orbitals in the plane of the ring (Walsh orbitals).³⁵ A p-orbital at an adjacent planar sp^2 atom is well aligned to interact with either member of the Walsh pair. This interaction leads to a small activation of methylene groups adjacent to cyclopropane rings toward H-atom abstraction³⁶ and is responsible for the small but significant stabilization energy of the cyclopropylmethyl radical (2.4 kcal mol⁻¹).³⁷ In radical **18a \cdot the NHC–BH unit is planar and its π -system can also align to interact with the cyclopropane Walsh orbitals.****

The DFT computed SOMO of model radical **18b \cdot (Figure 12 and Scheme 5) shows how the π -arrangement of the NHC–boryl unit extends into the plane of the three-membered ring giving a coherent π -system extended over the whole molecule. The calculated B–C_{3ring} bond length of 1.556 Å is significantly less than the analogous B–C bond length of the alkyl substituted **20a** (1.668 Å) and even slightly less than that of the aryl-substituted **4a \cdot (1.560 Å). The small $a(^{11}\text{B})$ observed for **18a \cdot is a consequence of the significant electron delocalization into the three-membered ring. The very small magnitude of the hfs from H $^\beta$ in radical **18a \cdot is also unusual. However, this is also explained by **18a \cdot adopting the delocalized structure shown in Figure 12. This places H $^\beta$ in the nodal plane of the SOMO so that its interaction with the unpaired electron is negligible.**********

To learn if the cyclopropyl group activates the adjacent BH₂ bonds, we carried out competitive H-abstraction experiments between **18a** and propan-2-ol as described above (see the



Figure 12. DFT computed structure and SOMO for cyclopropyl–boryl radical **18b \cdot .**

Scheme 5. Lack of Ring-Opening of the Ligated Cyclopropylboryl Radical **18a \cdot**

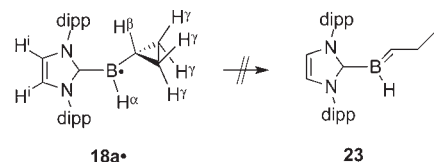


Table 6. EPR Parameters^a for NHC–B \cdot -alkyl Radicals

radical	T/K or DFT basis set	$a(^{11}\text{B})$	$a(1\text{H}^\alpha)$	$a(2\text{N})$	$a(2\text{H}^i)$	$a(1\text{H}^\beta)$	$a(2\text{H}^\gamma)$	$a(2\text{H}^\gamma')$
16\cdot		7.8	10.8	4.1	nr			
18a\cdot	290	4.5	9.0	4.2	~1.2	nr	~1.2	nr
18b\cdot	6-31G+(d)	10.3	-8.9	3.8	-1.0	0.2	1.1	-0.7
18b\cdot	EPR-iii	3.2	-8.3	2.4	-1.6	0.1	1.2	0.7

^a g -factors = 2.0030 ± 0.0005 . nr = not resolved.

Supporting Information). A rate constant ratio $k_{\text{H}}(\mathbf{18a})/k_{\text{H}}(i\text{-PrOH}) = 77.0$ was determined at 295 K. Use of the known²¹ rate constant for H-atom abstraction from propan-2-ol by *t*-BuO \cdot leads to $k_{\text{H}}(\mathbf{18a}) = 1.4 \times 10^8 \text{ M}^{-1} \text{ s}^{-1}$ at 295 K. This rate constant is the same as that for H-abstraction from the standard dipp-Imd-BH₃ **1**.¹⁴ If there is indeed a small activation of the BH₂ bonds in **18a** by the cyclopropyl group, then this is counter-balanced by increased steric shielding of the boron.

Cyclopropylcarbiny, cyclopropylaminy, and cyclopropyloxy radicals ring-open extremely rapidly to relieve ring strain.³⁷ However, the observation of the spectrum of **18a \cdot demonstrates that ring-opening of this ligated cyclopropylboryl radical to produce radical **23** does not occur even up to 350 K.³⁸ By using eq 1, we estimated that the activation energy for this ring-opening is >15.6 kcal mol⁻¹ and that the rate constant at 300 K is <40 s⁻¹. The reluctance of **18a \cdot to undergo β -scission is again a consequence of the instability of B=C double bonds. In agreement with this, a DFT computation [UB3LYP/6-31G+(d)] with the model *N,N'*-dimethylimidazol-2-ylidene analog **18b \cdot showed a strongly endothermic β -scission with only the shallowest of minima for the ring-opened radical, the latter having a distorted geometry (see the Supporting Information).******

CONCLUSIONS

Hydrogen atom abstraction by *t*-BuO \cdot radicals readily took place from the BH₂ groups of all of the second-generation B-aryl substituted NHC-boranes. Spin was extensively delocalized in the resulting radicals, which had SOMOs extending across the NHC, BH, and aryl units, thus making them bora-analogues of diphenylmethyl radicals. These NHC-B \cdot HAr radicals were substantially less reactive than NHC-BH₂ \cdot in abstracting Br-atoms from alkyl bromides, probably because of increased steric shielding of their radical centers.

Radicals **2a-c \cdot , with large dipp substituents pendent from the NHC groups, underwent dimerizations about 2 orders of magnitude slower than analogues without the B-aryl substituents, a consequence of the additional steric shielding. The evidence favored head-to-head coupling yielding ligated diborane derivatives rather than head-to-tail coupling through the aromatic ring of the substituent. In the case of the di-*t*-butyl-substituted complex **6**, a new type of ligated diboranyl radical, with a structure intermediate between that of a ligated diborane and a diborene, was generated from the head-to-head dimer.**

The behavior of B-alkyl-substituted NHC-boranes depended strongly on an interplay between the NHC-substituents and the B-substituents. For ligated boranes with large pendant dipp substituents, H-abstraction was directed away from boron to the alkyl groups. The resulting β -bora-alkyl radicals underwent exothermic β -scissions with production of dipp-Imd-BH₂ \cdot radical (**1**) and an alkene. The reverse reactions, that is, additions of NHC-BH₂ \cdot to simple alkenes, are projected to be unfavorable and endothermic, but addition of **3 \cdot to 1,1-diphenylethene does occur. In a remarkable example of the steric control achievable with NHC scaffolds, for the ligated borane with *N,N'*-diisopropyl substituents, the site of H-abstraction reverted to boron, and the alkyl-substituted-boryl radical was obtained.**

The B-cyclopropyl-NHC-boryl radical generated from **18a** displayed evidence of electron delocalization into the Walsh orbitals in the plane of the three-membered ring. Unlike other *c*-C₃H₅X \cdot radicals (X = CR₂, NR, O), this radical did not ring-

open even up to 350 K. This is a striking demonstration of the reluctance of B=C double bonds to form.

EXPERIMENTAL SECTION

Preparation and Characterization of the NHC-Boranes. See the Supporting Information.

EPR Spectroscopy. EPR spectra were obtained with a Bruker EMX 10/12 spectrometer fitted with a rectangular ER4122 SP resonant cavity and operating at 9.5 GHz with 100 kHz modulation. Stock solutions of each NHC-borane (2–15 mg) and DTBP (ca. 0.1 mL) in *tert*-butylbenzene or benzene (1.0 mL) were prepared and sonicated if necessary. An aliquot (0.2 mL), to which any additional reactant had been added, was placed in a 4 mm o.d. quartz tube, deaerated by bubbling nitrogen for 15 min, and photolyzed in the resonant cavity by unfiltered light from a 500 W super pressure mercury arc lamp. Solutions in cyclopropane were prepared on a vacuum line by distilling in the cyclopropane, degassing with three freeze-pump-thaw cycles, and finally flame sealing the tubes. Most of the EPR spectra were recorded with 2.0 mW power, 0.8 G_{pp} modulation intensity, and gain of ca. 10⁶. In all cases where spectra were obtained, hfs were assigned with the aid of computer simulations using the Bruker SimFonia and NIEHS Winsim2002 software packages. For kinetic measurements, precursor samples were used mainly in “single shot” experiments; that is, new samples were prepared for each temperature and each concentration to minimize sample depletion effects. In a few cases, second shot data were included. EPR signals were double integrated using the Bruker WinEPR software, and radical concentrations were calculated by reference to the double integral of the signal from a known concentration of the stable radical 2,2-diphenyl-1-picrylhydrazyl (DPPH) [1×10^{-3} M in PhMe], run under identical conditions, as described previously.³⁹

ASSOCIATED CONTENT

Supporting Information. Experimental details of the preparations of the boranes; NMR spectra of all new compounds; sample EPR spectra of NHC-boryl and related radicals; experimental and computed hfs of NHC-boryl radicals; kinetic data for NHC-boryl radical decays; details of photochemical reactions; and DFT-optimized geometries and energies for the NHC-boryl radicals. This material is available free of charge via the Internet at <http://pubs.acs.org>.

AUTHOR INFORMATION

Corresponding Author

jcw@st-andrews.ac.uk; curran@pitt.edu; emmanuel.lacote@icsn.cnrs-gif.fr

Present Addresses

^{||}ICSN CNRS, Bâtiment 27, Av. de la Terrasse, 91198 Gif-sur-Yvette Cedex, France.

ACKNOWLEDGMENT

This work was supported by grants from the U.S. National Science Foundation (CHE-0645998 to D.P.C.), from Agence Nationale de la Recherche (ANR, BLAN0309 Radicaux Verts, and 08-CEXC-011-01, Borane), UPMC, CNRS, and IUF (M.M., L.F.). Technical assistance (MS, elemental analyses) was generously offered by FR 2769. J.C.W. thanks EaStChem for financial support. We thank Jacques Lalevée for helpful discussions.

REFERENCES

- (1) (a) Kuhn, N.; Henkel, G.; Kratz, T.; Kreutzberg, J.; Boese, R.; Maulitz, A. H. *Chem. Ber.* **1993**, *126*, 2041–2045. (b) Ramnial, T.; Jong, H.; McKenzie, I. D.; Jennings, M.; Clyburne, J. A. C. *Chem. Commun.* **2003**, 1722–1723. (c) Yamaguchi, Y.; Kashiwabara, T.; Ogata, K.; Miura, Y.; Nakamura, Y.; Kobayashi, K.; Ito, T. *Chem. Commun.* **2004**, 2160–2161.
- (2) Ueng, S.-H.; Makhlof Brahmī, M.; Derat, É.; Fensterbank, L.; Lacôte, E.; Malacria, M.; Curran, D. P. *J. Am. Chem. Soc.* **2008**, *130*, 10082–10083.
- (3) (a) Weber, L.; Dobbert, E.; Stammler, H.-G.; Neumann, B.; Boese, R.; Bläser, D. *Chem. Ber.* **1997**, *130*, 705–710. (b) Matsumoto, T.; Gabbai, F. P. *Organometallics* **2009**, *28*, 4252–4253.
- (4) (a) Braunschweig, H.; Chiu, C.-W.; Radacki, K.; Kupfer, T. *Angew. Chem., Int. Ed.* **2010**, *49*, 2041–2044. (b) Monot, J.; Solovyev, A.; Bonin-Dubarle, H.; Derat, É.; Curran, D. P.; Robert, M.; Fensterbank, L.; Malacria, M.; Lacôte, E. *Angew. Chem., Int. Ed.* **2010**, *49*, 9166–9169.
- (5) Bissinger, P.; Braunschweig, H.; Kraft, K.; Kupfer, T. *Angew. Chem., Int. Ed.* **2011**, *50*, 4704–4707.
- (6) Ueng, S.-H.; Fensterbank, L.; Lacôte, E.; Malacria, M.; Curran, D. P. *Org. Lett.* **2010**, *12*, 3002–3005.
- (7) (a) Chu, Q.; Makhlof Brahmī, M.; Solovyev, A.; Ueng, S.-H.; Curran, D. P.; Malacria, M.; Fensterbank, L.; Lacôte, E. *Chem.-Eur. J.* **2009**, *15*, 12937–12940. (b) Lindsay, D. M.; McArthur, D. *Chem. Commun.* **2010**, 46, 2474–2476. (c) McArthur, D.; Butts, C. P.; Lindsay, D. M. *Chem. Commun.* **2011**, 47, 6650–6652.
- (8) Monot, J.; Makhlof Brahmī, M.; Ueng, S.-H.; Robert, C.; Desage-El Murr, M.; Curran, D. P.; Malacria, M.; Fensterbank, L.; Lacôte, E. *Org. Lett.* **2009**, *11*, 4914–4917.
- (9) (a) Tehfe, M.-A.; Monot, J.; Makhlof Brahmī, M.; Bonin-Dubarle, H.; Curran, D. P.; Malacria, M.; Fensterbank, L.; Lacôte, E.; Lalevé, J.; Fouassier, J.-P. *Polym. Chem.* **2011**, *2*, 625–631. (b) Tehfe, M.-A.; Makhlof Brahmī, M.; Fouassier, J.-P.; Curran, D. P.; Malacria, M.; Fensterbank, L.; Lacôte, E.; Lalevé, J. *Macromolecules* **2010**, *43*, 2261–2267.
- (10) (a) Rablen, P. R. *J. Am. Chem. Soc.* **1997**, *119*, 8350–8360. (b) Rablen, P. R.; Hartwig, J. F. *J. Am. Chem. Soc.* **1996**, *118*, 4648–4653.
- (11) Walton, J. C. *Angew. Chem., Int. Ed.* **2009**, *48*, 1726–1728.
- (12) Hioe, J.; Karton, A.; Martin, J. M. L.; Zipse, H. *Chem.-Eur. J.* **2010**, *16*, 6861–6865.
- (13) Ueng, S.-H.; Solovyev, A.; Yuan, X.; Geib, S. J.; Fensterbank, L.; Lacôte, E.; Malacria, M.; Newcomb, M.; Walton, J. C.; Curran, D. P. *J. Am. Chem. Soc.* **2009**, *131*, 11256–11262.
- (14) Walton, J. C.; Makhlof Brahmī, M.; Fensterbank, L.; Lacôte, E.; Malacria, M.; Chu, Q.; Ueng, S.-H.; Solovyev, A.; Curran, D. P. *J. Am. Chem. Soc.* **2010**, *132*, 2350–2358.
- (15) Solovyev, A.; Ueng, S.-H.; Monot, J.; Fensterbank, L.; Malacria, M.; Lacôte, E.; Curran, D. P. *Org. Lett.* **2010**, *12*, 2998–3001.
- (16) (a) Baban, J. A.; Marti, V. P. J.; Roberts, B. P. *J. Chem. Soc., Perkin Trans. 2* **1985**, 1723–1733. (b) Paul, V.; Roberts, B. P. *J. Chem. Soc., Perkin Trans. 2* **1988**, 1183–1193. (c) Baban, J. A.; Roberts, B. P. *J. Chem. Soc., Perkin Trans. 2* **1988**, 1195–1200. (d) Kirwan, N.; Roberts, B. P. *J. Chem. Soc., Perkin Trans. 2* **1989**, 539–550. (e) Dang, H. S.; Roberts, B. P. *Tetrahedron Lett.* **1992**, *33*, 6169–6172. (f) Dang, H. S.; Diart, V.; Roberts, B. P.; Tocher, D. A. *J. Chem. Soc., Perkin Trans. 2* **1994**, 1039–1045. (g) Roberts, B. P.; Steel, A. J. *J. Chem. Soc., Perkin Trans. 2* **1994**, 2411–2422. (h) Lucarini, M.; Pedulli, G. F.; Valgimigli, L. *J. Org. Chem.* **1996**, *61*, 1161–1164. (i) Barton, D. H. R.; Jacob, M. *Tetrahedron Lett.* **1998**, *39*, 1331–1334. (j) Sheeler, B.; Ingold, K. U. *J. Chem. Soc., Perkin Trans. 2* **2001**, 480–486.
- (17) Makhlof Brahmī, M.; Monot, J.; Desage-El Murr, M.; Curran, D. P.; Fensterbank, L.; Lacôte, E.; Malacria, M. *J. Org. Chem.* **2010**, *75*, 6983–6985.
- (18) Exner, O. In *Conformational Analysis in Chemistry*; Chapman, N. B., Shorter, J., Eds.; Plenum: New York, 1978; pp 439–540.
- (19) Frisch, M. J.; et al. *Gaussian 03*, revision A.1; Gaussian, Inc.: Pittsburgh, PA, 2003.
- (20) Previous work has shown computed $a(^{11}\text{B})$ values depend strongly on the basis set employed.
- (21) (a) Paul, H.; Small, R. D.; Scaiano, J. C. *J. Am. Chem. Soc.* **1978**, *100*, 4520–4527. (b) Malatesta, V.; Scaiano, J. C. *J. Org. Chem.* **1982**, *47*, 1455–1459.
- (22) We thank Mr. Andrey Solovyev for conducting this experiment.
- (23) (a) Wang, Y.; Quillian, B.; Wei, P.; Wannere, C. S.; Xie, Y.; King, R. B.; Schaefer, H. F., III; Schleyer, P. v. R.; Robinson, G. H. *J. Am. Chem. Soc.* **2007**, *129*, 12412–12413. (b) Wang, Y.; Quillian, B.; Wei, P.; Xie, Y.; Wannere, C. S.; King, R. B.; Schaefer, H. F., III; Schleyer, P. von R.; Robinson, G. H. *J. Am. Chem. Soc.* **2008**, *130*, 3298–3299.
- (24) See, for example: (a) Eisch, J. J. *Adv. Organomet. Chem.* **1996**, *39*, 355. (b) Berndt, A. *Angew. Chem., Int. Ed. Engl.* **1993**, *32*, 985–988.
- (25) Ueng, S.-H.; Fensterbank, L.; Lacôte, E.; Malacria, M.; Curran, D. P. *Org. Biomol. Chem.* **2011**, *9*, 3415–3420.
- (26) (a) Moezzi, A.; Bartlett, R. A.; Power, P. P. *Angew. Chem., Int. Ed. Engl.* **1992**, *31*, 1082–1083. (b) Moezzi, A.; Olmstead, M. M.; Power, P. P. *J. Am. Chem. Soc.* **1992**, *114*, 2715–2717. (c) Grigsby, W. J.; Power, P. P. *Chem. Commun.* **1996**, 2235–2236. (d) Grigsby, W. J.; Power, P. P. *Chem.-Eur. J.* **1997**, *3*, 368–375.
- (27) Scheschkewitz, D. *Angew. Chem., Int. Ed.* **2008**, *47*, 1995–1997.
- (28) Walton, J. C. *J. Chem. Soc., Perkin Trans. 2* **1998**, 603–605.
- (29) (a) Sabbe, M. K.; Reyniers, M.-F.; Van Speybroeck, V.; Waroquier, M.; Marin, G. B. *ChemPhysChem* **2008**, *9*, 124–140. (b) Sirjean, B.; Glaude, P. A.; Ruiz-Lopez, M. F.; Fournet, R. *J. Phys. Chem. A* **2008**, *112*, 11598–11610.
- (30) (a) Wong, M. W.; Pross, A.; Radom, L. *J. Am. Chem. Soc.* **1993**, *115*, 11050–11051. (b) Wong, M. W.; Pross, A.; Radom, L. *J. Am. Chem. Soc.* **1994**, *116*, 6284–6292. (c) Wong, M. W.; Pross, A.; Radom, L. *J. Am. Chem. Soc.* **1994**, *116*, 11938–11943.
- (31) Fischer, H.; Radom, L. *Angew. Chem., Int. Ed.* **2001**, *40*, 1340–1371.
- (32) Rosenstein, I. In *Radicals in Organic Synthesis*, 1st ed.; Renaud, P., Sibi, M., Eds.; Wiley-VCH: Weinheim, 2001; Vol. 1, pp 50–71.
- (33) Tiño, J.; Borsig, E.; Pilar, J. *Collect. Czech. Chem. Commun.* **1969**, *34*, 66.
- (34) (a) Newcomb, M. In *Radicals in Organic Synthesis*, 1st ed.; Renaud, P., Sibi, M., Eds.; Wiley-VCH: Weinheim, 2001; Vol. 1, pp 317–336. (b) Walton, J. C. In *Carbocyclic Three- and Four-Membered Ring Compounds*; de Meijere, A., Ed.; Georg Thieme Verlag: Stuttgart, 1997; Vol. E 17c of Houben Weyl, *Methoden der Organischen Chemie*, pp 2438–2525. (c) Nonhebel, D. C. *Chem. Soc. Rev.* **1993**, *22*, 347–359.
- (35) (a) Walsh, A. D. *Trans. Faraday Soc.* **1949**, *45*, 179. (b) Hoffmann, R. *J. Am. Chem. Soc.* **1968**, *90*, 1475–1485. (c) Hemmersbach, P.; Klessinger, M. *Tetrahedron* **1980**, *36*, 1337–1343.
- (36) Roberts, C.; Walton, J. C. *J. Chem. Soc., Chem. Commun.* **1984**, 1109–1111. (b) Ingold, K. U.; Walton, J. C. *Acc. Chem. Res.* **1986**, *19*, 72–77.
- (37) Walton, J. C. *Magn. Reson. Chem.* **1987**, *25*, 998–1000.
- (38) Even more dramatic changes in equilibrium constants between a closed shell bicyclic ring and a diradical have been observed by nuclear substitutions of borons for carbons in a bis-bora-analog of cyclobutane-1,3-diyl, see: Scheschkewitz, D.; Amii, H.; Gornitzka, H.; Schoeller, W. W.; Bourissou, D.; Bertrand, G. *Science* **2002**, *295*, 1880–1881.
- (39) Maillard, B.; Walton, J. C. *J. Chem. Soc., Perkin Trans. 2* **1985**, 443–450.